Kinetics of phase ordering in the O(*n*) model with a conserved order parameter

2001 J. Phys. A: Math. Gen. 34 3985

(http://iopscience.iop.org/0305-4470/34/19/303)

INSTITUTE OF PHYSICS PUBLISHING JOURNAL OF PHYSICS A: MATHEMATICAL AND GENERAL

J. Phys. A: Math. Gen. **34** (2001) 3985–4002 www.iop.org/Journals/ja PII: S0305-4470(01)21380-8

Kinetics of phase ordering in the O(n) model with a conserved order parameter

F Rojas[1], **Sanjay Puri**[2] **and A J Bray**[3]

[1] Centro de Ciencias de la Materia Condensada, UNAM, Apartado Postal 2681, Ensenada, Baja California 22800, Mexico
[2] School of Physical Sciences, Jawaharlal Nehru University, New Delhi 110067, India
[3] Department of Physics and Astronomy, The University, Manchester M13 9PL, UK

Received 19 January 2001

Abstract

We study the phase-ordering dynamics of the O(n) model with a conserved order parameter for systems with topological defects. We present results from both cell dynamical simulations and predictions of a Gaussian auxiliary field (GAF) approximation for the XY ($n = 2$) model in two and three dimensions, and the Heisenberg ($n = 3$) model in three dimensions. We describe the results for the structure factor $S(q)$ and growth law $L(t)$ from simulations. The growth laws obtained are consistent with theoretical predictions based on energy-scaling arguments. The structure factor shows good dynamical scaling using a length extracted from its first moment. The simulations are compared with the theoretical predictions of the GAF for the scaling functions. Our results show that the GAF gives a good qualitative description of most features of the structure factor. However, it overestimates the amplitude of the Porod tail in the large-q limit. Moreover, for small q, the structure factor exhibits a q^2-behaviour instead of the expected (generalized) Yeung result of q^4.

PACS numbers: 6460, 0510G, 0250E

1. Introduction

The ordering kinetics of systems described by a non-scalar order parameter has been of considerable interest in recent years [1]. The two main physical properties which characterize an ordering system are (a) the shape of the two-point correlation function or its Fourier transform, the structure factor, and (b) the time dependence of the characteristic length scale in the system. Now, it is well established that the correlation function $C(r, t)$ satisfies the dynamic scaling relation at late times, i.e.

$$C(r, t) = f(r/L(t)) \tag{1}$$

where r is the distance, t is time, f is the scaling function and $L(t)$ is the characteristic length scale.

0305-4470/01/193985+18$30.00

The goal of much previous work has been to determine these quantities both theoretically and numerically. The growth laws can be determined using heuristic arguments for the dynamics of defects, renormalization group methods [2] and, recently, through energy-scaling arguments [3], while approximate theories for the calculation of the correlation function are often based on the Gaussian auxiliary field (GAF) method [4]. The latter method has been extended to the O(n) model with a nonconserved order parameter [5].

The advantages and limitations of the GAF approach in the theoretical understanding of phase ordering have been widely discussed in recent years. Although the GAF approach provides a good semi-quantitative description of the pair correlation function for both nonconserved scalar and vector order parameters, we now know that when a more careful analysis is carried out it does not provide as accurate a description as first thought. An example of this is the so-called 'absolute test', in which one considers the GAF predictions for a certain higher-order correlation function (e.g. the two-point function of the squared field) in addition to the usual pair correlation function. Plotting one correlation function against the other eliminates all adjustable parameters. Using this approach, the approximate Gaussian predictions are not very good when compared with simulation results, according to the study performed by Blundell *et al* [6]. Moreover, the statistical properties of the auxiliary field m are not well approximated by a Gaussian function, particularly for small values of m [7].

It seems that some of the drawbacks of the Gaussian theory can be addressed by introducing 'post-Gaussian' approximations [8] that have the right properties. However, the corresponding theoretical predictions for systems with a conserved non-scalar order parameter are not completely known. The purpose of this paper is to study the conserved O(n) model with the objective of assessing the predictions of the GAF and comparing them with result of our simulations. Previous numerical studies of conserved O(n) models include the XY model in two [9, 10] and three dimensions [10, 11]. More recently, the conserved clock model, which shows a crossover between O(n) and scalar behaviour, has also been studied [12].

In previous work [13][4], we have utilized the GAF approach to study the conserved O(n) model in the $1/n$ approximation. However, a complete solution of the approximate equation for the scaling function, with no approximations beyond the GAF, was not possible at that stage.

In principle, the full solution for the approximate two-point correlation function which characterizes the phase-ordering dynamics in the conserved O(n) model should contain two important features. These are the conservation law, which is reflected in the vanishing of the structure factor when $q \to 0$; and the nature of the topological defects, which is reflected in a power-law behaviour ('Porod's law') of the tail of the structure factor.

In subsequent work [10], we developed an approach for solving the full GAF equation. This approach was based on an integration of the Laplacian operator using the corresponding Green function, as we shall elucidate shortly. The GAF solution was then compared with comprehensive computer simulations for the XY model [10].

In this paper we further examine the predictions of the GAF approach for conserved systems with topological defects, i.e. in systems with $n \leqslant d$, where d is the number of space dimensions, by extending and detailing the results presented in [10] to include the O(3) (Heisenberg) model in three dimensions. Thus we will focus on the study of systems with stable topological defects such as the XY model ($n = 2$) that supports vortex points (in $d = 2$) and vortex lines (in $d = 3$); and the Heisenberg model ($n = 3$) in $d = 3$ with monopole (or 'hedgehog') defects. The kinetics of these models is strongly influenced by

[4] Note that length scales in this paper differ by a factor of $8^{1/4}$ from those used here, due a different choice of scaling variable. The results quoted in this paper have been adjusted by this factor.

the interactions between defects. This paper provides analytical and numerical details of our somewhat terse presentation in [10]. Furthermore, we also present detailed numerical results for phase-ordering kinetics in the conserved O(3) (Heisenberg) model in $d = 3$, and compare these results with the predictions of the GAF approach.

In our simulations, we will primarily focus on the structure factor and its scaling properties. From the structure factor, one can extract information regarding relevant features such as the characteristic length scale $L(t)$; the conservation property; the large-q behaviour (generalized Porod law); and the small-q behaviour (the generalized Yeung result [1]: $S(q) \propto q^{\delta}$ as $q \to 0$, with $\delta = 4$).

The time dependence of the characteristic length scales for these systems has been predicted using an energy-scaling argument [3]. For the XY model in $d = 2$ one finds that $L(t) \sim t^{1/4}$, while $L(t) \sim (t \ln t)^{1/4}$ in $d = 3$. These two cases have been studied numerically through comprehensive CDS simulations in [10], and the lengths $L(t)$ obtained are consistent with the theoretical predictions.

For the conserved Heisenberg model in $d = 3$ the prediction obtained from energy scaling is $L(t) \sim t^{1/4}$. Our simulation results for this model, presented in this paper, yield $L(t) \sim t^{0.28}$, an exponent 12% larger than the theoretical prediction. However, we will demonstrate subsequently, through the analysis of a time-dependent effective exponent, that we have not reached the truly asymptotic regime of the dynamics. Nevertheless, the dynamical scaling of the structure factor in these models is reasonable if we use the reciprocal of the first moment of the spherically averaged structure factor, $S(k, t)$, as the scaling length, i.e. $L(t) = \langle k \rangle^{-1}$, where $\langle k \rangle = \int_0^\infty \mathrm{d}k\, kS(k, t) / \int_0^\infty \mathrm{d}k\, S(k, t)$.

This paper is organized as follows. Section 2 describes the main features of the approximate analytical theory for the scaling function. The procedure for reducing the nonlinear differential equation for the scaling function to an integro-differential equation is also presented. The XY model ($n = 2$) and the case of odd n are discussed separately. Section 3 presents details of our numerical simulations, while section 4 presents detailed numerical results for phase-ordering dynamics in conserved O(2) and O(3) systems with topological defects. These numerical results are compared to the analytical results obtained through the GAF approach in section 2. Finally, section 5 concludes this paper with a summary and discussion of our results in [10] and the present paper.

2. Gaussian auxiliary field approach

A successful approximate analytical method, which captures the main nonlinear features of phase ordering, is the GAF approach. This method provides a procedure for closing the equation of motion for the two-point correlation function, via the introduction of an auxiliary field which is smooth and has well defined statistical properties. The real field is related to the auxiliary field through a nonlinear mapping. With these elements, one can close the dynamical equation for the two-point one-time (or even two-time) correlation function.

A detailed derivation of the equations that define the GAF method for conserved vector fields can be found in [1]. Here, we provide a brief description of the method and present the main equations.

The starting point for this approach is the equation of motion for the conserved vector order parameter:

$$\frac{\partial \phi}{\partial t} = -\nabla^2 \left(\nabla^2 \phi - \frac{\partial V(\phi)}{\partial \phi} \right) \tag{2}$$

where the potential has the form $V(\phi) = \frac{1}{4}(1-\phi^2)^2$, with an equilibrium ground state with continuous O(n) symmetry, characterized by $|\phi| = 1$.

The idea is to eliminate the order parameter in favour of an auxiliary field $\boldsymbol{m}$, with specific statistical properties, through a mapping of the form $\phi = \boldsymbol{\sigma}(\boldsymbol{m})$. For systems with topological defects, the zeros of $\boldsymbol{m}$ define the positions of the defects, and $|\boldsymbol{m}|$ is a measure of distance to the topological defect. The standard procedure involves selecting the mapping that satisfies the equilibrium equation

$$\nabla_m^2 \phi = \frac{\partial V(\phi)}{\partial \phi} \tag{3}$$

where the equation is to be solved with the boundary conditions $\phi(0) = 0$, and $\phi(\boldsymbol{m}) \to \hat{\boldsymbol{m}}$ when $|\boldsymbol{m}| \to \infty$, where $\hat{\boldsymbol{m}}$ is a unit vector.

With this assumption, and using the statistical properties of the auxiliary field, one can obtain a closed equation of motion for the two-point, equal-time correlation function $C(r, t)$. To proceed, we first multiply equation (2) by the order parameter at another space point. Using the assumption that the auxiliary field can be approximated by a Gaussian distribution function, one can show that the equation of motion for C has the form

$$\frac{1}{2}\frac{\partial C}{\partial t} = -\nabla^2 \left(\nabla^2 C + \alpha(t)\, \gamma \frac{\mathrm{d}C}{\mathrm{d}\gamma} \right) \tag{4}$$

where $\alpha(t) = \langle m(1)^2 \rangle^{-1}$, the inverse of the second moment of any one component of $\boldsymbol{m}$ and $\gamma \equiv \gamma(12) = \langle m(1)m(2) \rangle / [\langle m(1)^2 \rangle \langle m(2)^2 \rangle]^{1/2}$ is the normalized two-point correlation function of m. For convenience in presentation, we have introduced the notation $1 \equiv \boldsymbol{r}_1$, $2 \equiv \boldsymbol{r}_2$ etc.

The relationship between C and γ for general n is obtained using the feature that the order parameter is a unit vector of the auxiliary field $\boldsymbol{m}$, except for a small region in the defect cores which is irrelevant in the scaling regime. Therefore one needs to determine the average $C(12) = \langle \hat{\boldsymbol{m}}(1) \cdot \hat{\boldsymbol{m}}(2) \rangle$. The necessary calculation was performed by Bray and Puri [14], and by Toyoki [15] (see also [5]), and the result (which we refer to as the 'BPT function') is

$$C = \frac{n\gamma}{2\pi} \left[B\left(\frac{n+1}{2}, \frac{1}{2} \right) \right]^2 F\left(\frac{1}{2}, \frac{1}{2}; \frac{n+2}{2}; \gamma^2 \right) \tag{5}$$

where $B(x, y)$ is the beta function and $F(a, b; c; z)$ is the hypergeometric function [16].

It is convenient to rewrite equation (4) in terms of the scaling variable $x = r/L(t)$, with $L(t) = (8t)^{1/4}$ (where the factor of eight is introduced for convenience). Requiring that all terms scale in the same way forces the relation $\alpha(t) = \lambda_d/(8t)^{1/2}$, where λ_d is recognized from our previous work [13] as one of the nonlinear eigenvalues.

Thus, the fourth-order, nonlinear differential equation for the scaling function $\gamma(x)$, obtained from (4), can be conveniently expressed as

$$x \frac{\mathrm{d}C}{\mathrm{d}x} = \nabla_x^2 \left[C_\gamma \left(\gamma'' + \frac{d-1}{x}\gamma' + \lambda_d \gamma + \frac{C_{\gamma\gamma}}{C_\gamma}(\gamma')^2 \right) \right] \tag{6}$$

where C_γ, $C_{\gamma\gamma}$ are the first and second derivatives of (5) with respect to γ, and the Laplacian operator with respect to the scaling variable is $\nabla_x^2 \equiv \frac{\mathrm{d}^2}{\mathrm{d}x^2} + \frac{d-1}{x}\frac{\mathrm{d}}{\mathrm{d}x}$, where d is the spatial dimension. If we explicitly evaluate all the terms in this equation, most of them are nonlinear and involve derivatives of C up to fourth order.

2.1. Poisson equation

In our early work on this problem [13], we were unable to solve the full equation for the correlation function (i.e. equation (6)), but presented only approximate solutions for the finite-

n cases. The difficulty involved in a direct numerical solution of (6) is principally related to the singularity at $\gamma = 1$, with the strongest singularity being associated with the fourth-order derivative $C_{\gamma\gamma\gamma\gamma}$. This term is obtained when ∇_x^2 operates on $C_{\gamma\gamma}$ on the right-hand side of (6). For $n = 2$, for example, $C_{\gamma\gamma\gamma\gamma} \sim (1-\gamma)^{-3}$ for $\gamma \to 1$. In this paper we present details of a method which overcomes this problem and makes the numerical procedure substantially easier. A preliminary report of this work has been presented in [10].

The approach that we use is to reinterpret equation (6) as a Poisson equation [17], so that we can perform a first integration using the Green function for the operator ∇_x^2. This procedure considerably simplifies the numerical solution of the nonlinear differential equation, which can be written as the following Poisson equation:

$$\nabla_x^2 \mu(x) = S(x). \tag{7}$$

In equation (7) the field $\mu(x)$ is defined by

$$\mu(x) = C_\gamma \left[\gamma'' + \frac{d-1}{x}\gamma' + \lambda_d \gamma + \frac{C_{\gamma\gamma}}{C_\gamma}(\gamma')^2 \right] \tag{8}$$

and the source $S(x)$ is an isotropic function that only depends on the magnitude of the scaling variable $x = |\boldsymbol{x}|$:

$$S(x) = x\frac{\mathrm{d}C}{\mathrm{d}x}. \tag{9}$$

The solution of equation (7) depends on the spatial dimension d. We limit our discussion to the two cases of interest, namely $d = 2, 3$. The Green function G is defined by the equation

$$\nabla_x^2 G(\boldsymbol{x}, \boldsymbol{x}') = -\delta(\boldsymbol{x} - \boldsymbol{x}') \tag{10}$$

and the solutions for $d = 2, 3$ are

$$G(\boldsymbol{x}, \boldsymbol{x}') = \begin{cases} \dfrac{1}{4\pi}\dfrac{1}{|\boldsymbol{x} - \boldsymbol{x}'|} & d = 3 \\ -\dfrac{1}{2\pi}\ln|\boldsymbol{x} - \boldsymbol{x}'| & d = 2. \end{cases} \tag{11}$$

Applying the inverse of the Laplacian operator to equation (7), its formal solution is

$$\mu(x) = -\int \mathrm{d}\boldsymbol{x}'\, G(\boldsymbol{x}, \boldsymbol{x}')\, S(|\boldsymbol{x}'|). \tag{12}$$

Because of the isotropy of the source S, the angular integration in (12) can be carried out leaving an integrand that just depends on the magnitudes $x = |\boldsymbol{x}|$ and $x' = |\boldsymbol{x}'|$. First let us consider the $d = 3$ case. (The corresponding result for $d = 2$ is derived in the appendix.) Performing the angular integration, we obtain

$$\mu(x) = -\frac{1}{2}\int_0^\infty \mathrm{d}x'\, \frac{x'}{x}\left(|x + x'| - |x - x'|\right) S(x'). \tag{13}$$

Further simplification can be achieved by dividing the domain of integration into the two intervals $[0, x]$ and $[x, \infty]$. Inserting the explicit form (9) for S, and integrating by parts using the boundary conditions $C(0) = 1$ and $C(\infty) = 0$, we find

$$\mu(x) = \int_0^x \mathrm{d}x' \left[\frac{3x'^2}{x} - 2x'\right] C(x') + 2\int_0^\infty \mathrm{d}x'\, x' C(x'). \tag{14}$$

The second integral is a constant, which is determined by taking the limit $x \to 0$. We identify this constant as $\delta_{d=3} = \mu(0) = 2\int_0^\infty \mathrm{d}x'\, x' C(x')$. For the case $d = 2$, we can proceed in a similar manner, using the appropriate Green function, and we also find a constant second integral.

The two cases can be combined, to finally express the full equation in the form

$$\mu(x) = \delta_d + I_d(x) \tag{15}$$

where δ_d is a constant that depends on d, and $I_d(x)$ is an integral that depends on both x and d. The explicit functional forms for the two cases are

$$I_d(x) = \begin{cases} \displaystyle\int_0^x \mathrm{d}x' \left[\frac{3x'^2}{x} - 2x'\right] C(x') & d = 3 \\ \displaystyle\int_0^x \mathrm{d}x'\, x'(1 - 2\ln x + 2\ln x')\, C(x') & d = 2. \end{cases} \tag{16}$$

It is clear that, in both cases, the function $I_d(x)$ tends to zero for $x \to 0$. Finally, we can write equation (15) in terms of the explicit definition of μ (from equation (8)):

$$\gamma'' + \frac{d-1}{x}\gamma' + \lambda_d\gamma + \frac{C_{\gamma\gamma}}{C_\gamma}(\gamma')^2 = \frac{1}{C_\gamma}\left(\delta_d + I_d(x)\right). \tag{17}$$

Thus, we have transformed the original problem of solving a fourth-order, nonlinear differential equation into the solution of an integro-differential equation which only involves second derivatives in both γ and C. Furthermore, the number of nonlinear terms has been reduced considerably. This substantial simplification of the equation makes it easier to find a numerical solution satisfying the correct boundary conditions. To find the solution, we use a standard numerical algorithm for solving differential equations, employing a trapezoidal algorithm to evaluate the integral $I_d(x)$ at each step. This procedure is possible because, by extracting the infinite integral δ_d explicitly, we have written the equation in a form in which the remaining integral $I_d(x)$ only requires function values $C(x')$ for $x' \leqslant x$, where x is the current value of the independent variable. We have checked that the procedure is stable and convergent, if we use a suitable step size in the integration routine.

As the integro-differential equation is equivalent to the original fourth-order equation, we expect it to represent a nonlinear eigenvalue problem, as discussed in previous work [10,13,17]. The eigenvalues are determined by using the asymptotic boundary conditions, which require the absence at large x of the two unphysical solutions (an increasing exponential and a constant) of the linearized equation [17]. Having determined the function γ with these properties, we substitute it into the BPT function (5) to obtain the correlation function for the field ϕ. We shall show in the following subsections, by analysing the small-x expansion of the solutions, that the problem is indeed defined in terms of only two adjustable parameters.

2.2. XY model: the case $n = 2$

We know that the XY model describes the dynamics of vortex points ($d = 2$) and vortex lines or strings ($d = 3$), which are the characteristic singular topological defects of a two-component field.

In order to solve equation (17), we first note that the function $\gamma(x)$ has a small-x expansion of the form

$$\gamma(x) = 1 - \frac{\alpha^2}{2}x^2 - \beta\frac{x^2}{\ln x} + \cdots \tag{18}$$

which may be verified by inserting this form into (17) using the form of $C(\gamma)$ valid for $\gamma \to 1$ obtained from (5).

Inserting the small-x form (18) in (17), and equating coefficients of leading (O(1)) and next-to-leading (O($1/\ln x$)) terms, yields the following relations between the parameters λ_d,

δ_d, α and β:

$$\lambda_d = d\alpha^2 \tag{19}$$

$$\delta_d = \alpha^2 + 2\beta d. \tag{20}$$

Using these results, we can eliminate λ_d and δ_d in terms of α and β in equation (17). The equation is then solved with initial conditions $\gamma(0) = 1$ and $\gamma'(0) = 0$, and the 'eigenvalues' (α, β) are determined by requiring a physically acceptable (i.e. decreasing) solution at large values of x.

2.3. The case with n odd

In this section we describe the corresponding treatment of the $n = 3$ model in $d = 3$, which can accommodate stable singular defects (monopoles, or 'hedgehogs'). The cases where the number of components of the order parameter is odd do not have any logarithmic singularities, so the analysis of the small-x expansion is considerably simpler. In this case, we expand the function $\gamma(x)$ only up to the quadratic term,

$$\gamma(x) = 1 - \frac{\alpha^2}{2}x^2 + \cdots \tag{21}$$

with the same boundary conditions (i.e. $\gamma(0) = 1$, $\gamma'(0) = 0$) as in the XY model.

We need to know the limit of C_γ when $x \to 0$ or, equivalently, when $\gamma \to 1$, to determine the x-dependence of the right-hand side in equation (17). Towards this end, we rewrite equation (5) using the transformation formulae of the hypergeometric function [16]:

$$C = \gamma F\left(\frac{1}{2}, \frac{1}{2}; \frac{2-n}{2}; 1-\gamma^2\right) + \frac{n\gamma}{2\pi}\left[\Gamma^2\left(\frac{n+1}{2}\right)\Gamma\left(-\frac{n}{2}\right)\right]\left[\Gamma\left(\frac{n+2}{2}\right)\right]^{-1} \times (1-\gamma^2)^{n/2} F\left(\frac{n+1}{2}, \frac{n+1}{2}; \frac{n+2}{2}; 1-\gamma^2\right). \tag{22}$$

Taking the derivative with respect to γ, one finds that C_γ approaches a constant as $\gamma \to 1$, given by

$$C_\gamma = \frac{n-1}{n-2}. \tag{23}$$

On the other hand, the corresponding nonlinear term on the left-hand side of equation (17) has the amplitudes

$$\frac{C_{\gamma\gamma}}{C_\gamma} \sim \begin{cases} (1-\gamma^2)^{-1/2} & n = 3 \\ \text{constant} & n \geqslant 5. \end{cases} \tag{24}$$

Introducing the above expressions into the differential equation, and equating the leading-order [O(1)] terms in the limit $x \to 0$, we obtain a relation between the parameters δ_d, λ_d and α:

$$\delta_d = \frac{n-1}{n-2}\left(\lambda_d - d\alpha^2\right). \tag{25}$$

This problem is also a double-eigenvalue problem but is now defined in terms of the parameters α and λ_d.

3. Details of numerical simulations

In our simulations we used an Euler discretization of equation (2) on a square or cubic lattice with periodic boundary conditions. The order parameter of the XY model is a two-component quantity, i.e. $\phi = (\phi_1(i,t), \phi_2(i,t))$, and the order parameter for the Heisenberg model has three components, i.e. $\phi = (\phi_1(i,t), \phi_2(i,t), \phi_3(i,t))$. The lattice sites are labelled by i, which is a two-component ($i = (x, y)$) or three-component ($i = (x, y, z)$) variable, depending on the dimensionality. According to the Euler discretization scheme, the vector field $\phi_{t+\Delta t}$ at time $t + \Delta t$ is related to the vector field ϕ_t at time t as follows:

$$\phi_{t+\Delta t}(i) = \phi_t(i) - \Delta_D \left[\Delta t \Delta_D \phi_t(i) + f_t\left(\phi_t(i)\right)\right] \tag{26}$$

with

$$f_t = \Delta t \phi_t (1 - \phi_t^2). \tag{27}$$

In equation (26), Δ_D represents a discrete lattice Laplacian. The numerical stability and performance of the algorithm is substantially improved by using an approximately isotropic Laplacian [18] which includes nearest- and next-nearest-neighbour sites.

Our simulations on the XY model in $d = 2$ used a mesh size $\Delta x = 1.70$ and a time step $\Delta t = 0.15$ on a lattice of size $(256)^2$. The spherically averaged structure factor was obtained as an average over 80 runs with independent random initial conditions. For the XY model in $d = 3$, we used a mesh size $\Delta x = 1.70$, a time step $\Delta t = 0.1$ and a lattice of size $(64)^3$. Structure-factor data were obtained as an average over 50 runs.

Our simulations of the Heisenberg model ($n = 3$) in $d = 3$ used a mesh size $\Delta x = 1.70$, and a time step $\Delta t = 0.20$. The system size was $(64)^3$ lattice sites and the dynamics was evolved up to dimensionless time $t_{\max} = 4000$. We computed the spherically averaged structure factor as an average over 50 independent runs.

The values for mesh size and time steps specified above guarantee a numerically stable procedure. However, we should stress at this point that the resultant numerical solution does not accurately represent the solution of the original partial differential equation (2). Rather, our Euler-discretized models should be understood in the spirit of cell dynamical system (CDS) models, which are computationally efficient models in the same dynamic universality class as the underlying partial differential equations [18]. Indeed, it would be hopelessly inefficient (and pointless) to attempt an accurate numerical solution of equation (2).

For the computation of the structure factor we use a 'hardened' order parameter field, normalized to the length of the fixed points of the dynamics. This procedure is useful to elucidate the large-k scaling behaviour ('Porod tail') of the structure factor, since it eliminates any signal from the 'soft' defect core by reducing the effective core size to zero. It has been demonstrated by Oono and Puri [19] that the fixed length scale associated with the soft defect cores can give rise to transient, nonuniversal features in structure-factor scaling plots for extended periods of time. The hardening procedure specified above eliminates these nonuniversal features by hand.

The structure factor is defined by

$$S(k, t) = \langle \phi(k, t) \cdot \phi(-k, t) \rangle \tag{28}$$

which, in the scaling regime, exhibits the dynamic scaling form

$$S(k, t) = [L(t)]^d g(kL(t)) \tag{29}$$

where g is the structure-factor scaling function. We will use the spherically averaged structure factor $S(k, t)$ to determine the characteristic length, defined by the reciprocal of the first moment

of the structure factor $L(t) \sim \langle k \rangle^{-1}$, where

$$\langle k \rangle = \frac{\int_0^{k_m} \mathrm{d}k\, k S(k,t)}{\int_0^{k_m} \mathrm{d}k\, S(k,t)}. \tag{30}$$

In equation (30), k_m is an upper cut-off, which we take as being half the magnitude of the largest wavevector in the Brillouin zone of the lattice.

4. Numerical results and discussion

4.1. XY model

Having described the GAF approach, which reduces the determination of the scaling function to the solution of a nonlinear eigenvalue problem, we now present detailed numerical results and compare these with the predictions of the GAF approach. In our simulations, we focused primarily on the computation of the structure factor, which exemplifies the salient features of the models discussed here.

Let us first consider the XY model in $d = 3$, which was investigated in [13] in the so-called 'O(C^3) approximation', in which the expansion of the function $\gamma\, \mathrm{d}C/\mathrm{d}\gamma$ appearing in (4) in powers of C is truncated at O(C^3). The results of this approximation provide a remarkably good fit to the real-space simulation results of Siegert and Rao [11], though the Porod tail in Fourier space is missing. Here we obtain the full GAF prediction, with its non-analytic small-x behaviour (which generates the Porod tail in momentum space), and the conservation law, and can now make a more meaningful comparison with simulation results. We show in this section that the solution to the full GAF equation (i.e. equation (17)) provides a reasonable description of the data for a simulation that (unlike [11]) uses hardened fields in the determination of the structure factor. Surprisingly, however, the real-space fit is noticeably poorer than for the O(C^3) approximation. The depth of the first minimum, for example, is much more accurately fitted by the latter approximation.

Figure 1 compares the GAF solution for the real-space scaling function, denoted by a solid line and with the abscissa rescaled such that the first zero is at $x = 1$, with the numerically obtained correlation function at dimensionless time $t = 5000$. It is clear that the agreement is quite good. The GAF solution has the small-x singular behaviour $f_{\mathrm{sing}}(x) \sim x^2 \ln(x)$. The eigenvalues determined for this solution take the approximate values $\alpha = 1.177\,567$ and $\beta = -0.155\,217$. The relevant geometrical features of $f(x)$, such as the positions of zeros and extrema, together with their amplitudes, are presented in table 1. The corresponding features obtained from the O(C^3) approximation are shown in brackets in table 1. Comparison with figure 1 shows that they fit the first minimum (and indeed the whole function [13]) rather better than the full GAF theory.

In Fourier space, we find that the GAF describes the numerical structure factor data rather well. In figure 2(a), plots of the scaled structure factor data and the GAF result (continuous curve) are presented. Good agreement between the Gaussian theory and the CDS simulations is evident. The log–log plot in figure 2(b) is more interesting because it shows the expected generalized Porod tail $g(q) \sim 1/q^5$. Recall that $g(q) \sim 1/q^{d+n}$ is the general result for a system with singular topological defects [14,15,20]. Both theory and data show this behaviour (which is absent in the O(C^3) approximation), but the GAF theory overestimates the amplitude of the power-law tail. This is more clearly seen in figure 2(c), which is a 'Porod plot' of the structure factor data of figure 2(a). However, the GAF approach qualitatively replicates all the main features (humps and valleys) of the data. Another feature present in the data is the expected

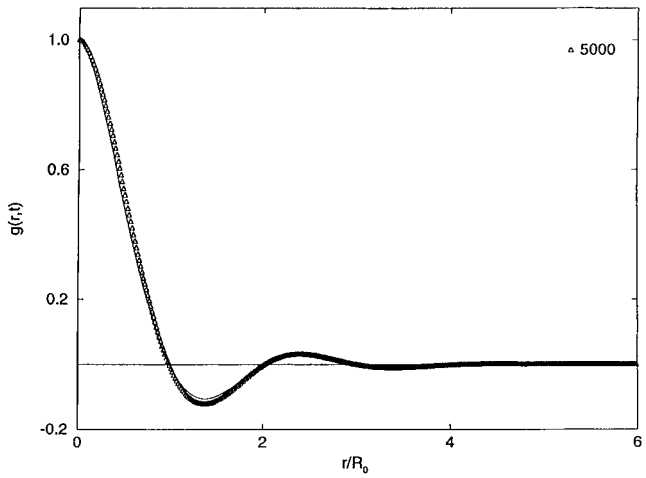

Figure 1. Scaling correlation function (solid curve) for the XY model (i.e. $n = 2$) in $d = 3$, determined using the GAF scheme described in the text. The data points are simulation data from [10].

Table 1. Nonlinear eigenvalues α and β, and zeros and turning points of the correlation scaling function, for the XY model in $d = 3$, within the GAF theory. Figures in brackets are the equivalent results for the $O(C^3)$ approximation (from [13]).

	$\alpha = 1.177\,567$	$\beta = -0.155\,217$
$n = 2, d = 3$	x	$f(x)$
First zero	1.5713(1.557)	0
First minimum	2.1742(2.154)	−0.104 926(−0.126 968)
Second zero	3.1722(3.122)	0
Second maximum	3.7636(3.710)	0.029 926(0.038 435)
Third zero	4.6869(4.611)	0
Second minimum	5.2540(5.175)	−0.009 235(−0.012 472)

q^4-behaviour for small q [1, 21]. This behaviour is *not* captured by the GAF theory, which gives a q^2-behaviour at small q.

Next, we consider the XY model in $d = 2$. Figure 3 is analogous to figure 1, and compares the GAF result (solid curve) with the numerical results for time $t = 10\,500$. It is clear that the agreement of the GAF results with the simulations is not as good as for $d = 3$. Again, the depth of the first minimum, and the height of the following maximum, are underestimated by the full GAF theory. The eigenvalues for the GAF solution take the approximate values $\alpha = 1.297\,719$ and $\beta = -0.269\,97$. To complete the geometrical analysis, table 2 details relevant numerical features of the scaling function. For fixed number of components ($n = 2$), we observe that both the value of α and the absolute value of the depth of the first minimum decreases when d increases. The corresponding data for the $O(C^3)$ approximation are shown in brackets. Comparison with figure 3 shows that they again describe the first minimum and the subsequent maximum quite well.

We proceed to a discussion of Fourier-space results and a comparison with simulation results for the structure factor. As in the case of the correlation function, the fit of the corresponding GAF solution to the data is noticeably worse than for $d = 3$, as can be observed in figure 4(a). The log–log plot of the same data (figure 4(b)) also reveals the q^4-result for

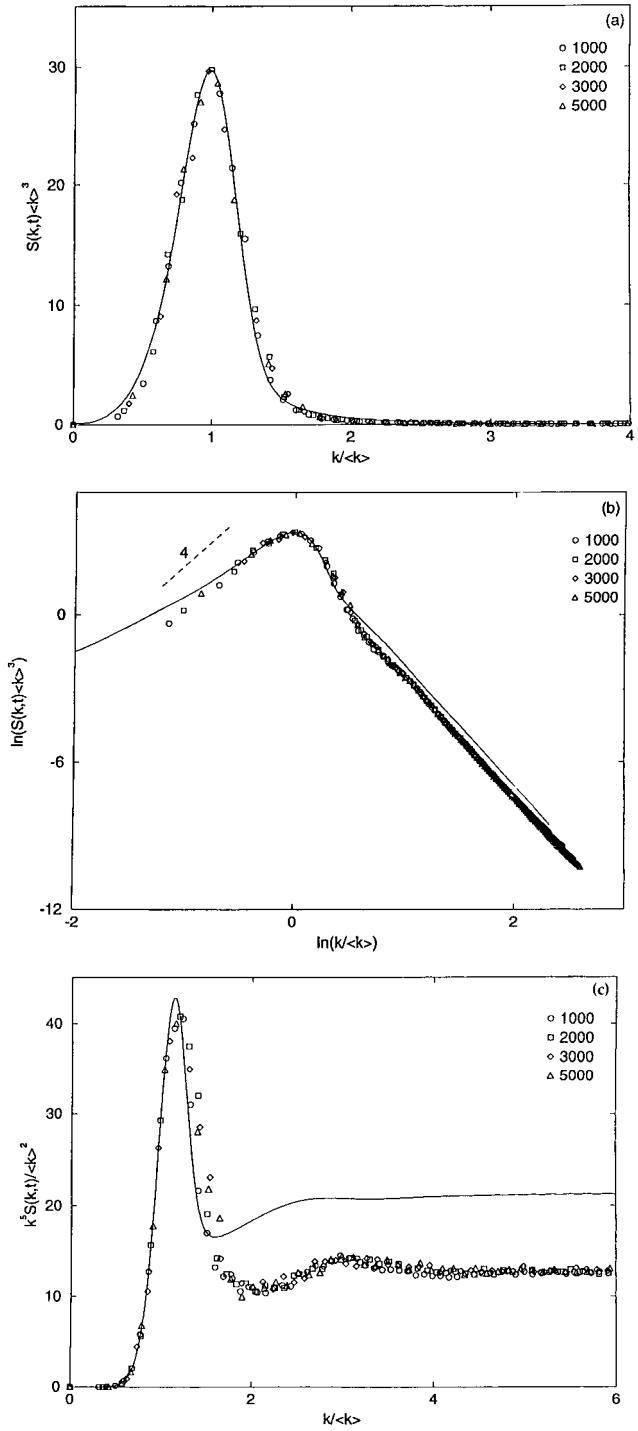

Figure 2. Scaled structure factor for $n = 2$, $d = 3$, for four different times: (*a*) linear–linear plot; (*b*) log–log plot; (*c*) Porod plot. The continuous curves are obtained from the numerical Fourier transform of the scaling function for the pair correlation function, calculated using the GAF scheme. The dashed line in (*b*) has slope four.

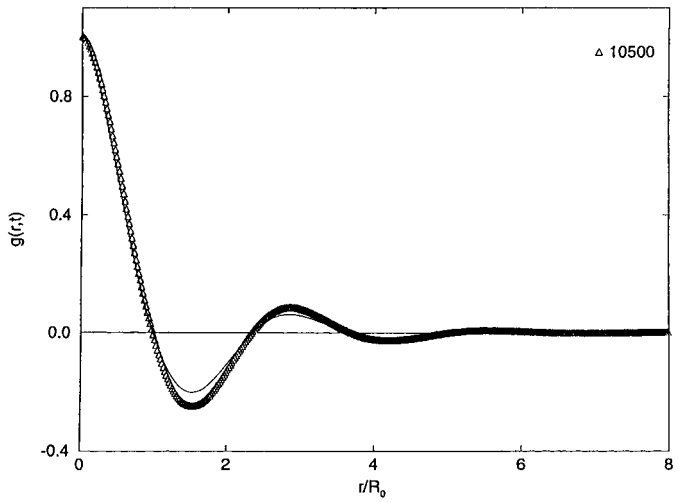

Figure 3. Scaling correlation function (solid curve) for the XY model in $d = 2$, determined using the GAF scheme. The data points are simulation data from [10].

Table 2. Nonlinear eigenvalues α and β, and zeros and turning points of the correlation scaling function, for the XY model in $d = 2$, within the GAF theory. Figures in brackets are the equivalent results for the O(C^3) approximation.

	$\alpha = 1.297\,719$	$\beta = -0.269\,97$
$n = 2, d = 2$	x	$f(x)$
First zero	1.278(1.249)	0
First minimum	1.960(1.914)	−0.201 981(−0.257 00)
Second zero	3.011(2.885)	0
Second maximum	3.652(3.518)	0.063 603(0.09413)
Third zero	4.631	0
Second minimum	5.233	−0.019 916

small q that is not reproduced by the Gaussian theory. The Porod tail is clearly displayed in the curve, but the theory again overestimates its amplitude. Figure 4(c) is a Porod plot of the same data. We conclude that the predictions of the Gaussian approximation for the $d = 2$ case are not as good as for $d = 3$. The theory is qualitatively correct, but does not provide either the correct amplitude for the Porod tail, or the correct small-q behaviour.

4.2. Heisenberg model

The numerical solution of the GAF equation for the real-space scaling function $f(x)$ for the Heisenberg model in $d = 3$ is presented in figure 5. The corresponding nonlinear eigenvalues take the approximate values $\alpha = 1.185\,168$ and $\lambda = 4.449\,264$. The relevant geometrical information of turning points and zeros for this function is provided in table 3. One aspect that we can observe, comparing the result for $f(x)$ with the GAF solution for the XY model in $d = 3$ is that, for fixed d, the absolute value of the amplitude for the first minimum and the eigenvalue α increase with n.

Next, we proceed to describe the results in Fourier space, both for the simulations and the theoretical approximation, which allows us to test the predictions of the Gaussian closure

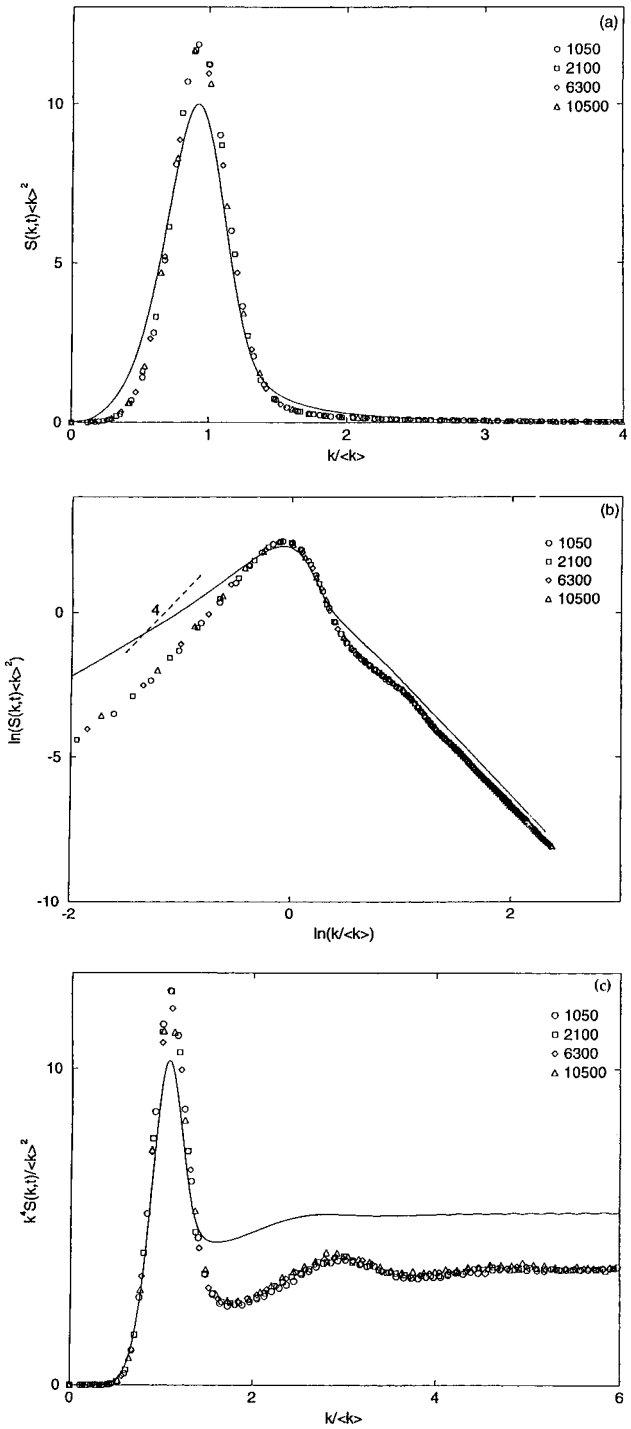

Figure 4. The same as figure 2, but for $d = 2$, i.e. (*a*), (*b*) and (*c*) are linear–linear, log–log and Porod plots of the scaled structure factor respectively, and the continuous curves are the GAF prediction.

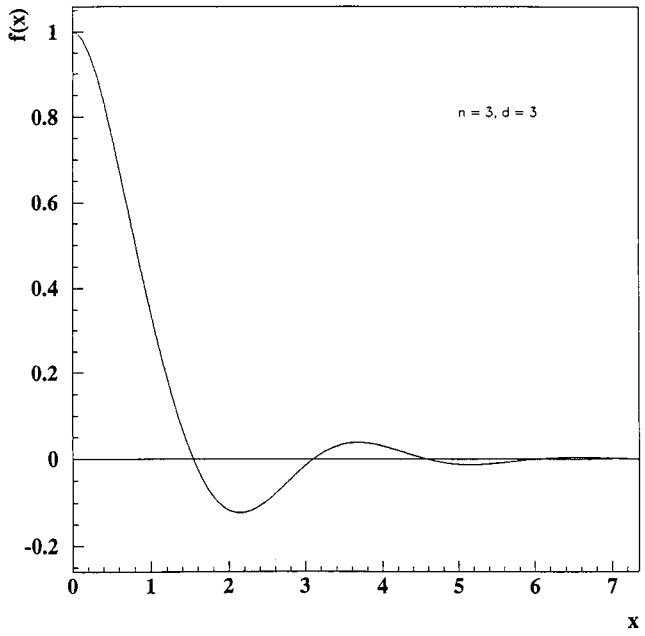

Figure 5. Real-space scaling function for the Heisenberg ($n = 3$) model in $d = 3$ from the GAF method.

Table 3. Nonlinear eigenvalues α and λ, and zeros and turning points of the correlation scaling function, for the Heisenberg model in $d = 3$, within the GAF theory.

	$\alpha = 1.185\,168$	$\lambda = 4.449\,264\,59$
$n = 3,\ d = 3$	x	$f(x)$
First zero	1.546	0
First minimum	2.142	−0.122 857
Second zero	3.102	0
Second maximum	3.688	0.037 787
Third zero	4.582	0
Second minimum	5.146	−0.012 45

scheme for the Heisenberg model. The results for the scaled structure factor are shown in figure 6(a). We observe that the numerical data exhibit reasonable dynamical scaling. The result of the GAF approach is shown by a solid curve. Again, we see that the agreement between the GAF solution and the numerical results is not particularly good.

The log–log plot in figure 6(b) is more interesting because it reveals the small-q and large-q behaviour of the structure factor scaling function $g(q)$. For small q, the simulations show the expected q^4-regime, consistent with the predictions for conserved systems with a vector order parameter [1], which extend the result obtained for scalar cases [21]. This power does not appear in the approximate theory, which gives a q^2-behaviour, as discussed before.

In the large-q regime, evidence of the expected Porod tail $g(q) \to A_{n=3}/q^6$ is clearly displayed. This tail is a consequence of the singular topological defects (i.e. monopoles) present in the system. The GAF solution, denoted by a solid curve, has this feature built in, but the tail amplitude is again overestimated. This point is further emphasized in a Porod plot of the data (figure 6(c)). The Porod plot also shows the existence of a hump around $q = 3$,

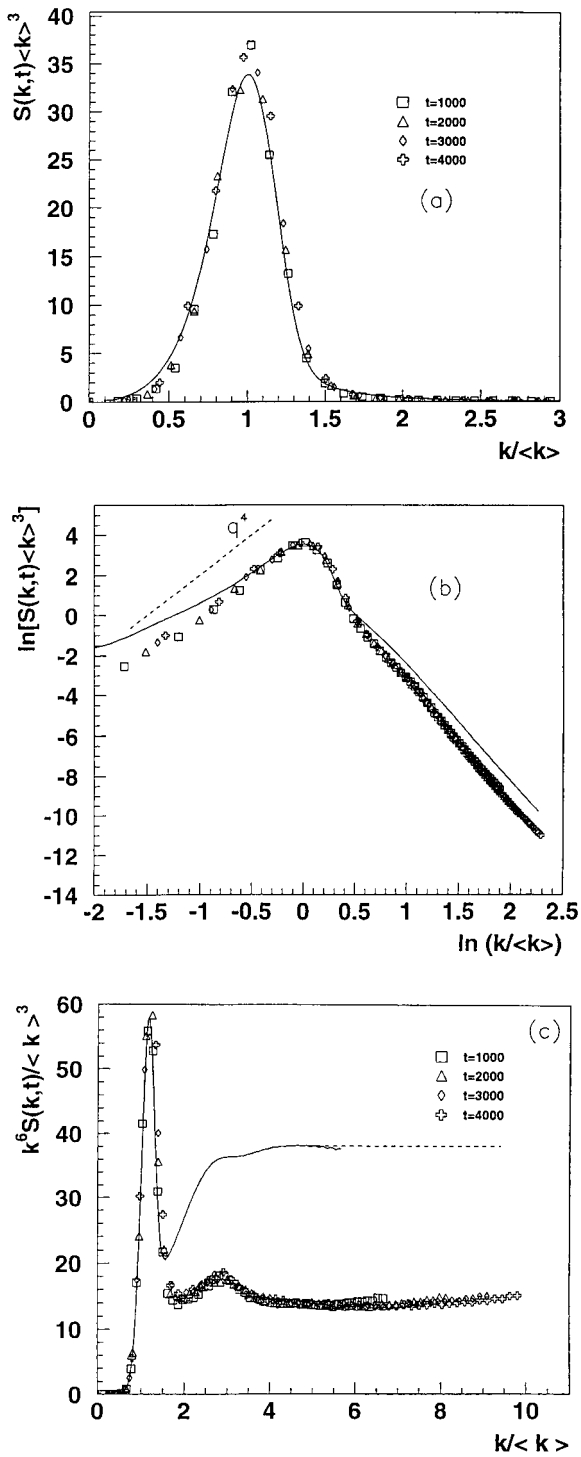

Figure 6. The same as figures 2 and 4, but for the three-dimensional Heisenberg ($n = 3$) model.

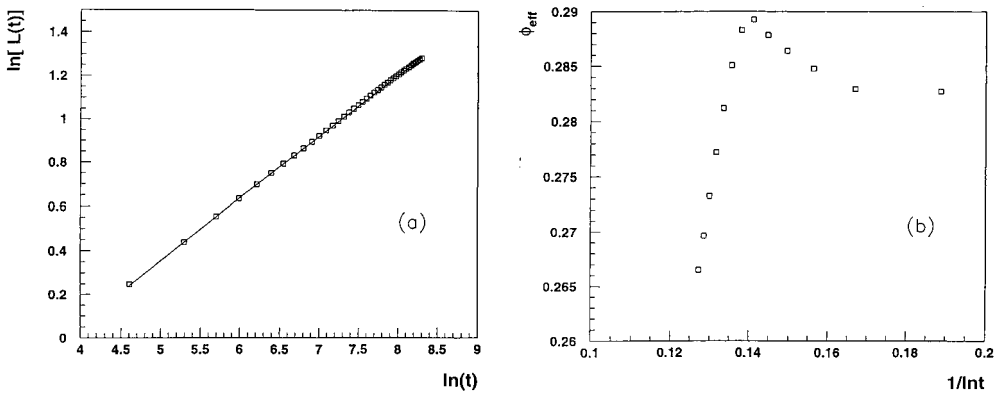

Figure 7. (*a*) Characteristic length $L(t)$ for the Heisenberg model in $d = 3$, extracted from the first moment of the structure factor; (*b*) effective exponent, $\phi_{\rm eff} \equiv \ln[L(at)/L(t)]/\ln(a)$, for $a = 1.5$.

similar to the effect seen in the XY models in $d = 2, 3$.

We have already discussed the time dependence of the characteristic length scale for the conserved XY model in $d = 2, 3$ in [10]. For brevity we focus here only on the time dependence of the length scale for the conserved Heisenberg model in $d = 3$. Figure 7(*a*) is a log–log plot of the simulation data for this length, defined, as usual, by $L(t) = \langle k \rangle^{-1}$. Assuming a simple power law of the form $L(t) = At^{\phi}$, we find that the best-fit value for the exponent is $\phi = 0.28$, some 12% larger than the value of one-quarter deduced from theoretical considerations [1,3]. We believe that the difference from the theoretical value is a consequence of our simulations not having accessed the truly asymptotic regime, for which longer runs are required. To test this idea we consider the time evolution of an effective exponent defined by $\phi_{\rm eff}(t) = \ln[L(at)/L(t)]/\ln(a)$ with $a = 1.5$. Figure 7(*b*) shows this effective exponent, which decreases at late times but has not yet reached an asymptotic value. Therefore, we believe that our present simulations are consistent with the theoretically predicted exponent $\phi = 1/4$, though they certainly fall short of providing conclusive evidence for it.

5. Summary

In summary, we have studied the predictions of the GAF approach to the non-equilibrium phase ordering of conserved systems with a vector order parameter. We have compared the theoretical GAF predictions with numerical simulations using CDS models for systems with singular topological defects, namely the XY model in $d = 2$ and 3 and the Heisenberg model in $d = 3$.

The functional forms of the scaled correlation function and structure factor for the XY model in $d = 3$ are well described by the GAF result, but in the other two cases the fit is not particularly good. Even for the $d = 3$ XY model, moreover, the cruder O(C^3) approximation [13] gives a better real-space fit. It would be interesting to understand the reasons for this. The numerical data exhibit good scaling for the structure factor, using the length scale $\langle k \rangle^{-1}$ extracted from the structure factor data. The numerical scaling function is characterized by the generalized Porod tail, expected from theoretical considerations [14, 15]. This important feature is missing from the O(C^3) approximation [13]. The numerical scaling function behaves as $g(q) \sim q^4$ for scaled wavevector $q \to 0$. This is in conformity with the proposed generalization to vector systems [1] of the (same) small-q result for scalar systems

with conserved order parameter [21].

The GAF predictions are not as good quantitatively as the corresponding predictions for non-conserved vector systems [22]. We found that the theory overestimates the amplitudes of the Porod tail, and the expected q^4-behaviour for small q is absent, with a q^2-behaviour found instead. Even though the theory is not quantitatively correct, it provides a reasonable qualitative description: the Porod tail and conservation are built in, and the theory replicates most of the qualitative features of the scaling forms of the correlation function and structure factor.

As far as the time dependence of the characteristic length scale is concerned, we have only presented here a numerical result for the Heisenberg model in $d = 3$. Our previous paper [10] had already presented detailed numerical results for the XY model in $d = 2, 3$. For the Heisenberg model, the numerical data suggest that the characteristic length obeys a growth law $L(t) \sim t^{0.28}$, with a mean exponent somewhat larger than the theoretical prediction [3] of one-quarter, but there is good evidence that the asymptotic regime has not been reached, with the effective exponent decreasing at later times.

Our main conclusion is that further refinements of the theory are needed to capture more precisely the salient features of the scaled structure factor. Going beyond the Gaussian approximation for the auxiliary field is an obvious starting point, and some steps in this direction have been attempted recently for scalar fields [8]. It seems likely that these methods can be extended to nonconserved vector fields [23]. In our view, extensions of the GAF theory for conserved fields must give priority to incorporating the correct q^4-behaviour at small q.

Acknowledgments

FR thanks CONACYT (Mexico) for financial support. SP and FR thank the Department of Physics and Astronomy of the University of Manchester, where this work was initiated, for hospitality, and the Isaac Newton Institute, Cambridge, where part of this work was done. This work was supported by the Engineering and Physical Sciences Research Council (UK).

Appendix. The XY model in $d = 2$

In this appendix, we calculate the function $I_2(x)$ given in equation (16), and the constant δ_2 in equation (15). We start from equation (12) for the case $d = 2$:

$$\mu(x) = -\frac{1}{2\pi} \int \mathrm{d}\boldsymbol{x}'\, S(|\boldsymbol{x}'|) \ln(\boldsymbol{x} - \boldsymbol{x}'). \tag{A.1}$$

Performing the angular integration gives

$$\mu(x) = \int_0^\infty \mathrm{d}x'\, x' S(x') [\theta(x - x') \ln x + \theta(x' - x) \ln x'] \tag{A.2}$$

$$= \int_0^x \mathrm{d}x'\, x' S(x') \ln x + \int_x^\infty \mathrm{d}x'\, x' \ln x' S(x'). \tag{A.3}$$

Using the definition (9) of the source S in terms of the derivative of the correlation function C, and carrying out an integration by parts, we obtain the final expression

$$\mu(x) = \int_0^x \mathrm{d}x'\, x' C(x') (1 - 2 \ln x + 2 \ln x')) + \delta_2 \tag{A.4}$$

where the constant $\delta_2 = \mu(0) = -\int_0^\infty \mathrm{d}x'\, x' C(x') (1 + 2 \ln x')$.

References

[1] For a recent review see: Bray A J 1994 *Adv. Phys.* **43** 357
[2] Bray A J 1989 *Phys. Rev. Lett.* **62** 2841
Bray A J 1990 *Phys. Rev.* B **41** 6724
[3] Bray A J and Rutenberg A D 1994 *Phys. Rev.* E **49** R27
Rutenberg A D and Bray A J 1995 *Phys. Rev.* E **51** 5499
[4] Mazenko G F 1989 *Phys. Rev. Lett.* **63** 1605
Mazenko G F 1990 *Phys. Rev.* B **42** 4487
[5] Liu F and Mazenko G F 1992 *Phys. Rev.* B **45** 6989
Bray A J and Humayun K 1992 *J. Phys. A: Math. Gen.* **25** 2191
[6] Blundell R E, Bray A J and Sattler S 1993 *Phys. Rev.* E **48** 2476
[7] Yeung C, Oono Y and Shinozaki A 1994 *Phys. Rev.* E **49** 2693
[8] Mazenko G F 1994 *Phys. Rev.* E **49** 3717
[9] Mondello M and Goldenfeld N 1993 *Phys. Rev.* E **47** 2384
[10] Puri S, Bray A J and Rojas F 1995 *Phys. Rev.* E **52** 4669
[11] Siegert M and Rao M 1993 *Phys. Rev. Lett.* **70** 1956
[12] Puri S, Ahluwalia R and Bray A J 1997 *Phys. Rev.* E **55** 2345
[13] Rojas F and Bray A J 1995 *Phys. Rev.* E **51** 188
[14] Bray A J and Puri S 1991 *Phys. Rev. Lett.* **67** 2670
[15] Toyoki H 1992 *Phys. Rev.* B **45** 1965
[16] Abramowitz M and Stegun I A 1970 *Handbook of Mathematical Functions* (New York: Dover)
[17] Mazenko G F 1991 *Phys. Rev.* B **43** 5747
[18] Oono Y and Puri S 1987 *Phys. Rev. Lett.* **58** 836
Oono Y and Puri S 1988 *Phys. Rev.* A **38** 434
Puri S and Oono Y 1988 *Phys. Rev.* A **38** 1542
[19] Oono Y and Puri S 1988 *Mod. Phys. Lett.* B **2** 861
[20] Bray A J and Humayun K 1993 *Phys. Rev.* E **47** 3191
[21] Yeung C 1988 *Phys. Rev. Lett.* **61** 1135
See also Furukawa H 1989 *J. Phys. Soc. Japan* **58** 216
Furukawa H 1989 *Phys. Rev.* B **40** 2341
Tomita H 1991 *Prog. Theor. Phys., Osaka* **85** 47
Fratzl P, Lebowitz J L, Penrose O and Amar J 1991 *Phys. Rev.* B **44** 4794
[22] See, e.g., Blundell R E and Bray A J 1994 *Phys. Rev.* E **49** 4925
[23] Mazenko G F Private communication